PILOT PERFORMANCE AND HEAT STRESS ASSESSMENT SUPPORT USING A COCKPIT THERMOREGULATORY SIMULATION MODEL

Jörg Schminder* , Robert Hällqvist** , Magnus Eek** , Roland Gårdhagen*
*Applied Thermodynamics and Fluid Mechanics, Linköping University, Linköping, Sweden
, **Systems Simulation and Concept Design, Saab Aeronautics, Linköping, Sweden

Keywords: *Thermal Comfort, Heat Stress, Thermoregulatory Model, Modeling and Simulation*

Abstract

Flights with high thermal loads inside the cockpit can have a considerable impact on pilot physiological and psychological performance resulting in thermal discomfort, dehydration and fatigue. In this work, a Functional Mock-up Interface (FMI) based aircraft system simulator is utilized with intent to compute and predict thermal comfort. The simulator can for example serve pilots as a tool for heat stress and flight risk assessment, supporting their pre-flight planning or be used by engineers to design and optimize cooling efficiency during an early aircraft design phase. Furthermore, the presented simulator offers several advantages such as map based thermal comfort analysis for a complete flight envelop, time resolved mental performance prediction, and a flexible composability of the included models.

1 Introduction

Thermal comfort describes a state in which humans sense a pleasant and satisfying environmental temperature [1]. A deviation from this state leads in hot environments to a feeling of being febrile, which goes gradually along with sweating, dehydration and lapse of concentration [2] [3]. Pilots of small aircraft with limited cooling performance as well as high performance aircraft with large transparent canopies are, during ground and low altitude flights, more often exposed to high heat loads when the weather conditions are hot and sun radiation is high. The significant increase of cockpit air temperature in helicopters and fixed wing airplanes, plus the resulting decline of thermal comfort under such hot conditions, is documented in several studies [4] [5]. The feeling of thermal discomfort, along with the awareness of potential heat illnesses, arises relatively distinctly in hot environments. However, physiological and mental performance may also decrease during long flight missions in moderate temperatures, easily underestimated by the pilot.

The objective of this study is to demonstrate how an Aircraft System Simulator (ASS) can support engineers, pilots, and ground crews to predict possible heat stress related hazards before a flight so that error awareness is increased, sufficient and energy efficient cooling is provided, and human health is not endangered. This is done by applying the Functional Mock-up Interface (FMI) standard [6] in order to enable a flexible integration of relevant sub-systems.

2 Method

One purpose of the ASS, schematically described in Fig.1, is to enable studies of thermal comfort coupled to Environmental Control System (ECS) overall performance. Interoperability between the modeled sub-systems is established via the FMI standard. Three novel models jointly describing the aggregated cockpit thermal comfort

conditions are connected to the ASS [7] [8]. The ASS is not aligned to a specific aircraft type but intended to be of research and industrial complexity in terms of range of application, non-linearities, and level of detail. The extensions and refinements of the ASS, relevant for detailed analyses of pilot thermal comfort, are described in this section. Available atmospheric boundary conditions are presented in section 2.1. The modeled sub-systems that together explicitly describe the provision of conditioned cockpit comfort air are described in section 2.2. Sub-systems modeling thermal comfort are over viewed in section 2.3.

2.1 Atmosphere

The atmosphere model (Fig.1c) provides all sub-models within the ASS with atmosphere data. The model includes to date three atmospheric representations: the International Standard Atmosphere (ISA) [9], the (suggested) International Tropical Atmosphere (ITRA) [10], and the Military Standard MIL-STD-210 [11].

2.2 Environmental Control

The environmental control related sub-system models (Fig.1b) described here are developed in Dymola and OpenModelica [12] [13], applying the object-oriented and equation based Modelica language. The aircraft engine model is intended to provide bleed air, extracted from the rear stages of the jet engine's compressor to the ECS model. The bleed air temperature and pressure are modeled as functions of Mach number, altitude, and prevailing ambient conditions.

The applied environmental control system model is a virtual representation of an ECS typically installed in a fighter aircraft [14] [15]. The ECS provides pressurized air at the needed mass flow, pressure, and temperature, to the cockpit, avionics, and pilot's garment. The engine bleed air supplied to the ECS is decreased in temperature by the primary heat exchanger. A bootstrap cooling system, the cooling pack, is used to further condition the air. This is achieved by means of a

compressor, a turbine, a series of heat exchangers, and a water separator. The implemented heat exchangers utilize ram air for refrigeration. The temperature and pressure of the ECS output air are controlled to specification by means of an incorporated controlling software, denoted ECS Control in Fig.1b. The implemented software controls the motorized valves, which in turn regulate the flow through two different cooling pack by-pass branches. [7] and [8] provide more detailed information about the model.
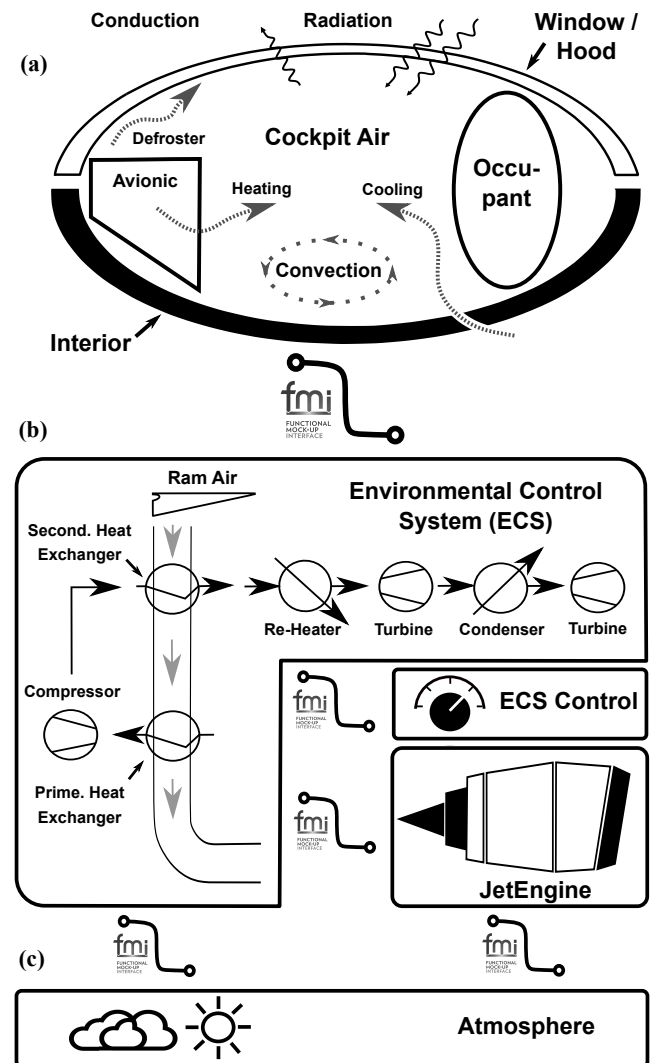
Fig. 1 : Concept diagram of the presented aircraft system simulator. Links between models illustrate schematically FMI interfaces. **(a)** cockpit thermal climate model and heat exchange mechanism, **(b)** environmental control model and its sub-systems, **(c)** the atmosphere model.

2.3 Cockpit Comfort

The Cockpit Thermal Climate/Comfort (CTC) model (Fig.1a) is an enhanced version of the original model [16] implemented in Matlab®. The model is currently running in a Simulink® environment and consists of three major sub-models: the cockpit model, the thermal comfort model, and the occupant model.

The cockpit model computes the temporal thermal conditions within the cockpit compartment with boundary conditions defined both by the ECS and the atmosphere model. The model consists of three smaller sub-models: the window/hood, the interior and the compartment air model. The hood model utilizes an energy balance, which in its general form reads

$$\dot{E}_{net} = \dot{E}_{cond} + \dot{E}_{conv} + \dot{E}_{rad} \ . \qquad (1)$$

Eq.(1) is then discretized using an explicit finite difference approach to compute the heat transfer through the transparent cockpit canopy. While conduction ($\dot{E}_{cond}$), convection ($\dot{E}_{conv}$), sun radiation, and other radiation ($\dot{E}_{rad}$) only occur at the surface nodes, internal nodes are only effected by conduction and sun radiation. Hence, for internal nodes Eq.(1) can be expressed as

$$\frac{\partial T}{\partial t}\rho c_p = \frac{\partial}{\partial x}\left(k\frac{\partial T}{\partial x}\right) + \dot{E}_{sun} \ . \qquad (2)$$

Both the interior and the cockpit air sub-model also make use of energy balances,

$$\dot{Q}_{int} = \dot{Q}_{int_{rad}} + \dot{Q}_{equip} + \dot{Q}_{occu} \\ - \dot{Q}_{int_{conv}} - \dot{Q}_{cool} \qquad (3)$$

$$\dot{Q}_{air} = \dot{Q}_{equip} + \dot{Q}_{occu} + \dot{Q}_{int_{conv}} + \dot{Q}_{def} \\ + \dot{Q}_{w_{conv}} - \dot{Q}_{vent} \ , \qquad (4)$$

to compute their respective change in temperature and use for time advancement

$$T^{t+dt} = T^t + \dot{Q}\frac{dt}{mc_p} \ . \qquad (5)$$

The interior, which includes all solid material (e.g. seats and panels), exchanges heat via radiation $\dot{Q}_{int_{rad}}$ and convection $\dot{Q}_{int_{conv}}$ with the surrounding cockpit air plus the cockpit's hood, Eq.(3). Major sources of heat to the interior can be the heat generated by the incident sun radiation, the equipment (instruments, computers) $\dot{Q}_{equip}$ and the aircrew's body heat $\dot{Q}_{occu}$. To regulate the temperature of the interior cooling air $\dot{Q}_{cool}$, provided by the ECS, is implemented as a heat sink. The cockpit air, Eq.(4), is mainly heated-up by convection between the air and interior $\dot{Q}_{int_{conv}}$. Additional heat sources are the equipment $\dot{Q}_{equip}$, the occupants $\dot{Q}_{occu}$, as well as the defroster air $\dot{Q}_{def}$ if activated. Cockpit air temperature can be controlled by ventilation air $\dot{Q}_{vent}$ coming from the ECS entering directly to the cockpit.

Thermal comfort prediction is enabled by modeling the cockpit wet-bulb and black-globe temperatures which together form, with cockpit dry-air temperature the input for several heat stress indices e.g. Wet Bulb Globe Temperature (WBGT) [17], Fighter Index of Thermal Stress (FITS) [18] or the Predicted Mean Vote (PMV) [19]. Than other indices like the Predicted Percentage of Dissatisfied (PPD) occupants can be deduce [20]. As previously presented for the interior and the cockpit air, wet-bulb and black-globe temperatures are computed applying energy balances

$$\dot{Q}_{bg} = \dot{Q}_{rad} + \dot{Q}_{conv} \qquad (6)$$

$$\dot{Q}_{nwb} = \dot{Q}_{rad} + \dot{Q}_{conv} - \dot{Q}_{evap} \ , \qquad (7)$$

which consider the radiative $\dot{Q}_{rad}$ as well as convective $\dot{Q}_{conv}$ heat exchange at the thermometers. Since the surface of the wet bulb thermometer is humid, an additional term had to be added including the heat loss due to evaporation $\dot{Q}_{evap}$. The temperature of both thermometers were subsequently advanced in time just as presented in Eq.(5). A more detailed description of how the models are implemented can be found in [16].

The physiological and psychological parameters

in this work are based on empirical regression models, found in the literature, utilizing cockpit environmental parameters and/or thermal comfort indices. Equilibrium rectal temperature (T_{rec}) is based on experimental data published by Lind [21] and is estimated by means of

$$T_{rec} = 0.000001T_{eff}{}^5 - 0.0001T_{eff}{}^4 \\ +0.004T_{eff}{}^3 - 0.06T_{eff}{}^2 \quad (8) \\ +0.46T_{eff} + 36.22$$

describing rectal temperature as a function of Effective Temperature (T_{eff}).

Mean Skin Temperature (T_{skin}) is computed as

$$T_{skin} = 0.1263T_{os} + 30.03 \quad (9)$$

at which T_{os} is the temperature of the cockpit air close to the pilot's body [22] calculated as

$$T_{os} = 0.8367T_c + 5.8 \ . \quad (10)$$

In addition, Song [22] published a linear regression to estimate the sweat rate (SR) of cockpit occupants,

$$SR = 12.13T_{os} - 149.96 \ . \quad (11)$$

Mean Metabolic Rate (MR) and Heart Rate (HR) are estimated as

$$MR = 0.04T_c{}^2 - 1.96T_c + 86.42 \quad (12)$$

$$HR = 0.05T_c{}^2 - 2.2T_c + 103.42 \quad (13)$$

at which only regressions, presented by Lou [23], for a clothing insulation of 0.9 clo are applied, since fighter cockpit pilots normally are almost completely covered by clothes.

Relative Task Performance (TP) Eq.(14) is computed by

$$TP = 0.0000623T_c{}^3 - 0.0058274T_c{}^2 \\ +0.1647524T_c - 0.4685328 \quad (14)$$

employing a curve fit, presented by Seppänen [24], setting task productivity in relation to indoor ambient temperature (T_c).

To get a notion of human error risk due to sub-optimal thermal conditions, the Unsafe Behavior Index (UBI) for light workload was chosen. The index is calculated as

$$UBI = 0.0008T_{wbgt}{}^2 - 0.0341T_{wbgt} \\ +0.5829 \quad (15)$$

and indicate the detrimental effect on the safety-related behavior in relation to WBGT [25].

2.4 Model Intercommunication

The models included in the presented simulator are exported as compressed model executables, according to the FMI standard format, where they are referred to as Functional Mock-up Units (FMUs). The environmental control sub-models, explained in section 2.2, are exported as FMUs from the commercially available Modelica tool Dymola® [12] [13]. The models comprising the CTC sub-models are ported from Matlab® to Simulink® via the "User-Defined Function block". The Dassault developed toolbox "FMI Kit For Simulink" [26] is subsequently used to generate FMUs from the resulting Simulink models.

The ASS is then implemented in two different integrating tools, Dymola® and the OM-Simulator. For the presented steady state simulations, the CTC models are incorporated as FMUs in the Dymola implementation; however, the Modelica models are kept in their original format. Transient simulations were executed in the open-source tool OMSimulator. The OMSimulator is a simulation environment supporting the FMI standard under development in the research collaboration Open Cyber Physical System Model-Driven Certified Development (OpenCPS) project [27]. In contrast to the steady state simulation, all of the modeled sub-systems

are incorporated as FMUs in this second implementation.

3   Results

The presented results are obtained by applying the ASS to compute the thermal conditions inside the cockpit. This is then used to estimate the physiological as well as psychological impact on the pilot. The simulated aircraft is a single-seater generic fighter comparable to a AJ37 (Viggen) or F-18 (Hornet). First, 40 steady state case simulations, each 800 s long, at different flight speeds and altitudes were simulated covering the entire flight envelope typical for an aircraft in this class [28] [29]. The atmospheric boundary conditions during the simulations correspond to a standard day defined by the international standard atmosphere (ISA).

Cockpit temperature (Fig.2a), computed by the CTC model, shows a variation of $40°C$ within the flight envelop and rises up to $125°C$ in regions with high Mach numbers. Cockpit air condition, provided by the ECS, offers the pilot a minimum air temperature (Fig.2b) of $0°C$ over a wide rage of the flight envelope, but rises easily up to $95°C$ during fast flights at low altitudes. The thermal comfort a pilot would experience within the flight envelope is assessed by four different indices. WBGT (Fig.2c) varies between $15°C$ and $30°C$ but reaches highly critical values above $33°C$ [17] outside the flight envelopes. FITS (Fig.2d) is below $33°C$ in a large part of the flight domain indicating no significant heat stress risk for the pilot. PMV (Fig.2e) of the present thermal situation varies from cold (-3) to hot (+3) resulting in PPD values (Fig.2f) from thermal neutral (0%) up to distinct dissatisfaction (100%).

The pilot's skin temperature (Fig.3a) is directly affected by the climatic in the the cockpit and varies between $32°C$ and $36°C$ inside the flight envelope, but exceeds $36°C$ rapidly beyond the borders. A Sweat rate (Fig.3b) of 100 g/m^2h-200 $g/m^2h$ is dominating within the flight envelop, but reaches considerably higher values in areas with high cockpit temperatures. The metabolic rate of the pilot (Fig.3c) is estimated as 60 W/m^2 in the operational area of the aircraft. However, higher rates are predicted outside the flight domain. The computed heart rate (Fig.3d) is, with some exceptions at high speed and high altitude flights, relatively constant at 70-80 BPM within the reference borders. The relative task performance (Fig.3e) is 100% in large parts of the flight envelop but falls quickly below 50% where the ECS has difficulties to provide the necessary cooling. The effect of the cockpit temperature on the pilot's safe work behavior (Fig.3f) shows with 16%-40% a low to moderate risk for unsafe actions within the assumed flight limits.

In addition to the steady state case simulation, a transient mission was simulated with the aim to demonstrate the bidirectional dynamic interaction of the FMI combined ECS and CTC model setup. The simulated mission includes four flight phases: take off, landing, and two cruise segments. The results focus on the 11 min long stepped-cruise part of the mission (Fig.4a) with both changes in altitude and flight speed.

To ensure thermal comfort during flight the ECS uses FITS (Fig.4b) as feedback input to regulate air-condition temperature. The ECS was programed to hold FITS constant at $20°C$, which was accomplished most of the time with exception during the fast, high speed decent where $27°C$ is exceeded. At the beginning of the cruise phase cockpit temperature lies around $22°C$ but increases temporally up to $38°C$ when quickly descending to lower altitudes. Subsequently, when level flight is established again, cockpit air temperature is stabilizing around $26°C$. Cooling air supplied by the ECS is initially maintained at $20°C$; however, a deviation from the set point is observed during the descent. After reaching level flight and reduced speed, cooling air drops down to an average value of $15°C$ to restore the anticipated value of $20°C$ FITS.
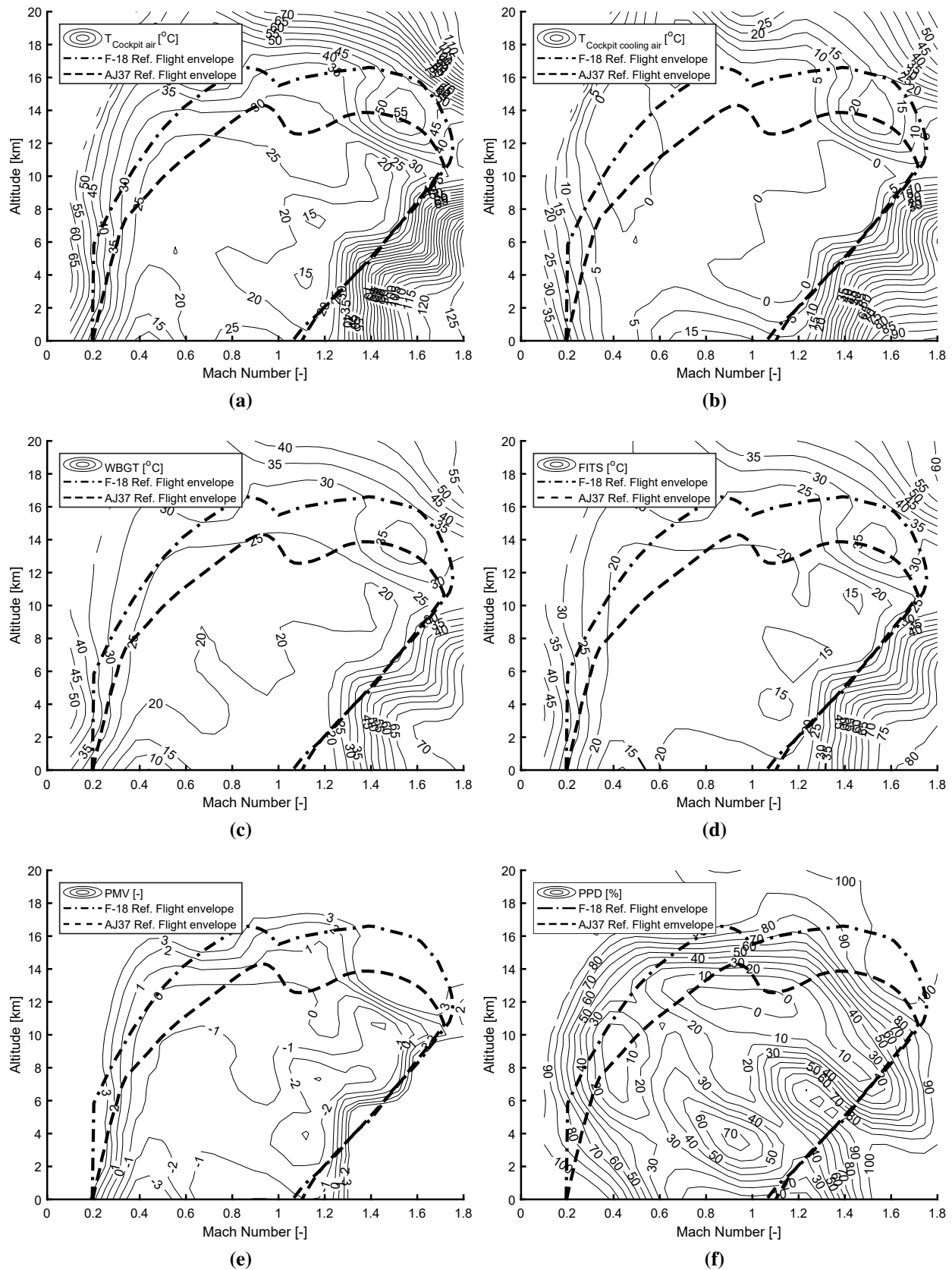
Fig. 2 : Steady state case simulation of cockpit temperatures and resulting thermal comfort within a potential flight envelope. (a), cockpit air temperature inside the flight envelope is in average below 30°C. **(b)**, ECS provided cooling air temperature increase significantly at higher Mach numbers. **(c)**, WBGT shows low to moderate heat stress risk within the envelope. **(d)**, FITS indicates no thermal risk inside the flight limits. **(e)**, PMV assess the thermal comfort as slightly chilly within the envelope. **(f)**, PPD varies considerably inside the borders.

(a)

(b)

(c)

(d)

(e)

(f)
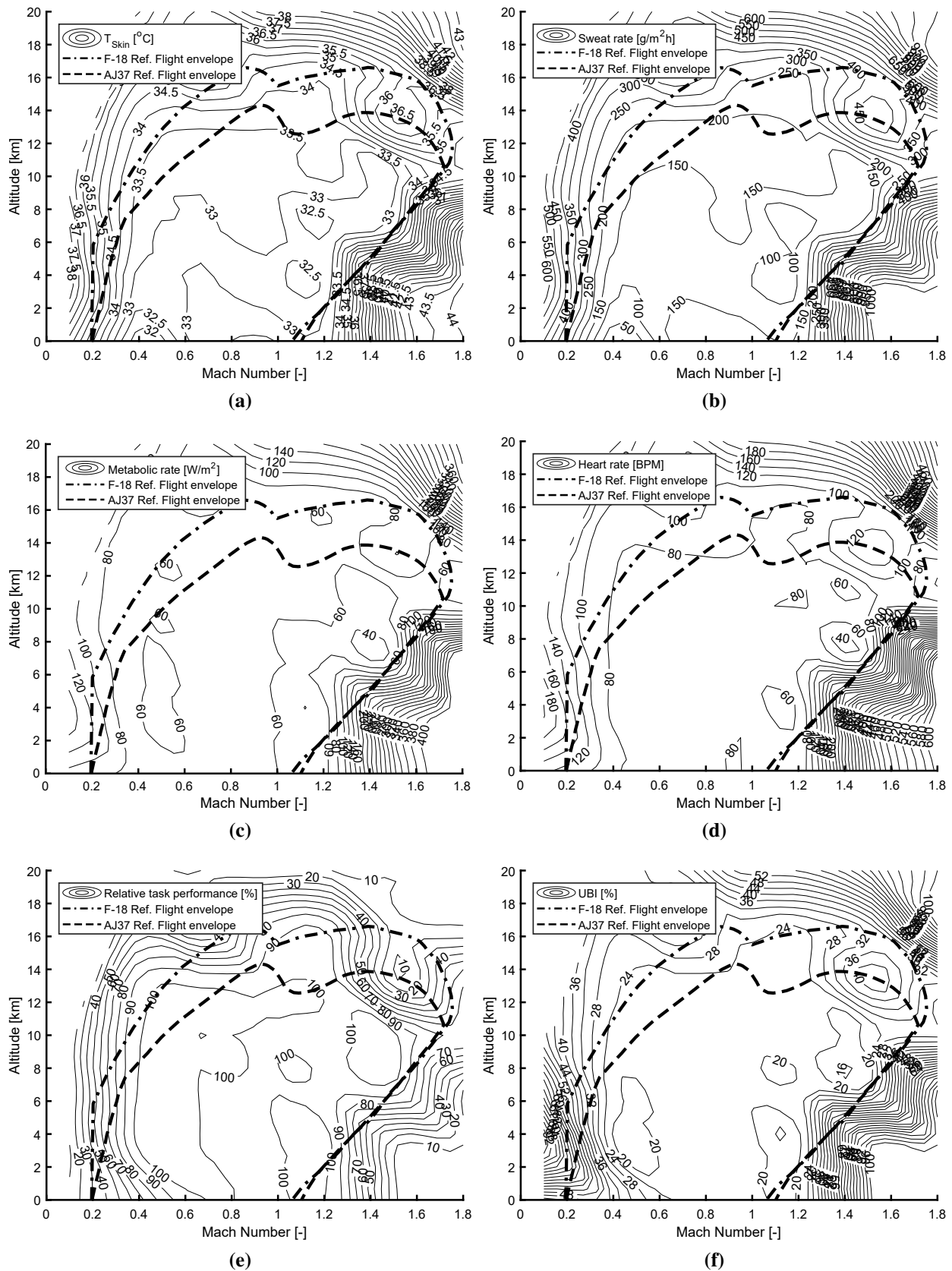
Fig. 3 : Steady state case simulation of pilot physiological and psychological parameters within a potential flight envelope. **(a)**, skin temperature inside flight envelope $\approx 34°C$. **(b)**, sweat-rate is with 450 g/m^{2}h clearly increased at high altitudes and Mach numbers. **(c)**, metabolic-rate within the envelope mostly ≈ 60 W/m^2. **(d)**, heart-rate ≈ 80 BPM mostly constant inside the limits. **(e)**, relative task performance is 100% inside the envelops. **(f)**, risk for unsafe work behavior increases rapidly outside the flight limits.

The computed rectal temperature (Fig.4c) remains constant at around 37°C during the flight, while skin temperature varies with ca. 2°C leading to an average of 33.2°C.

The change in estimated heart rate (Fig.4d) due to increased cockpit temperature amounts to 12.6 BPM between its maximum and minimum. The predicted relative task performance of the pilot does not fall below 97% when cockpit temperature is close to the defined comfort set-point, however it drops significantly (75%) when the cockpit temperature is increased.

4   Discussion

Ensuring thermal comfort during flight also means an increase in safety. To put this aspect into the focus of pilots and engineers, a simulation tool was presented providing important environmental, physiological and psychological information to support their flight planning, risk management and decision making. In addition, the study presents the potential of applying the FMI standard for interdisciplinary and cross-program-linguistic model-exchange and co-simulation.

Mapping vital aircraft system and aircrew parameters over the entire flight envelope, as presented in Fig.2 and Fig.3, facilitates a heliocentric view of man and machine performance and helps to identify potential hazards. The presented steady state simulations show (within the presumed performance limits illustrated by the reference flight envelops) good and reasonable results. Beyond the borderlines, where ECS works off design, performance decreases rapidly (Fig.2b) leading to an increase of cockpit air temperature (Fig.2a). This goes along with a significant decline in thermal comfort (Fig.2c-Fig.2f) where WBGT exceeds its maximum [17], FITS recommend to cancel planned flights [18], PMV indicates a too hot environment, and PPD shows a significant dissatisfaction with the prevailing cockpit climate [20]. Though all indices asses a clear discomfort for the occupants outside the envelop,

the PPD indicates also a moderate dissatisfaction with the prevailing thermal comfort inside the flight limits. One reason for this could be that PMV asses the cockpit climate as somewhat chilly.

The thermal conditions have a direct impact on the aircrews' physiology and mental performance (Fig.3). Within the reference flight envelope, human body parameters like skin temperature (Fig.3a), sweat rate (Fig.3b), metabolic rate (Fig.3c), and heart rate (Fig.3d) indicate no remarkable health risk. The picture looks rather different outside the envelopes where the cockpit temperature is high. The body tries to maintain a constant core temperature by utilizing sweat and vasodilation, which is supported by the increased sweat and heart rate [30]. In addition to the physiological impact concentration and attention is decreasing. The relative task performance (Fig.3e) is in large areas within the flight envelop predicted as high leading to a low risk for unsafe work behavior (Fig.3f). Outside the performance limits of the aircraft relative task performance drops significantly resulting in an increased risk for unsafe work behavior which in turn could lead to an enhanced probability for pilot error.

Regulating cockpit comfort can be done manually (by the pilot) or fully automatic. In the second scenario cockpit air temperature is typically measured and used as reference input for the ECS to adjust the cockpit climate if necessary. Controlling thermal comfort only by dry air temperature; however, this is not enough if the goal is to achieve pilot thermal comfort. The computed FITS was for this reason applied to regulate the ECS. The advantage of using a thermal comfort index as a control input is that these indices usually consider additional factors like humidity, radiation, air speed, etc. For the dynamic case (Fig.4) cockpit comfort is over the entire flight ensured since FITS stays below the suggested caution zone of 32°C (Fig.4b).
The physiology of the pilot is directly affected by the climate of the cockpit whereby predicted rectal and skin temperature (Fig.4c) as well as
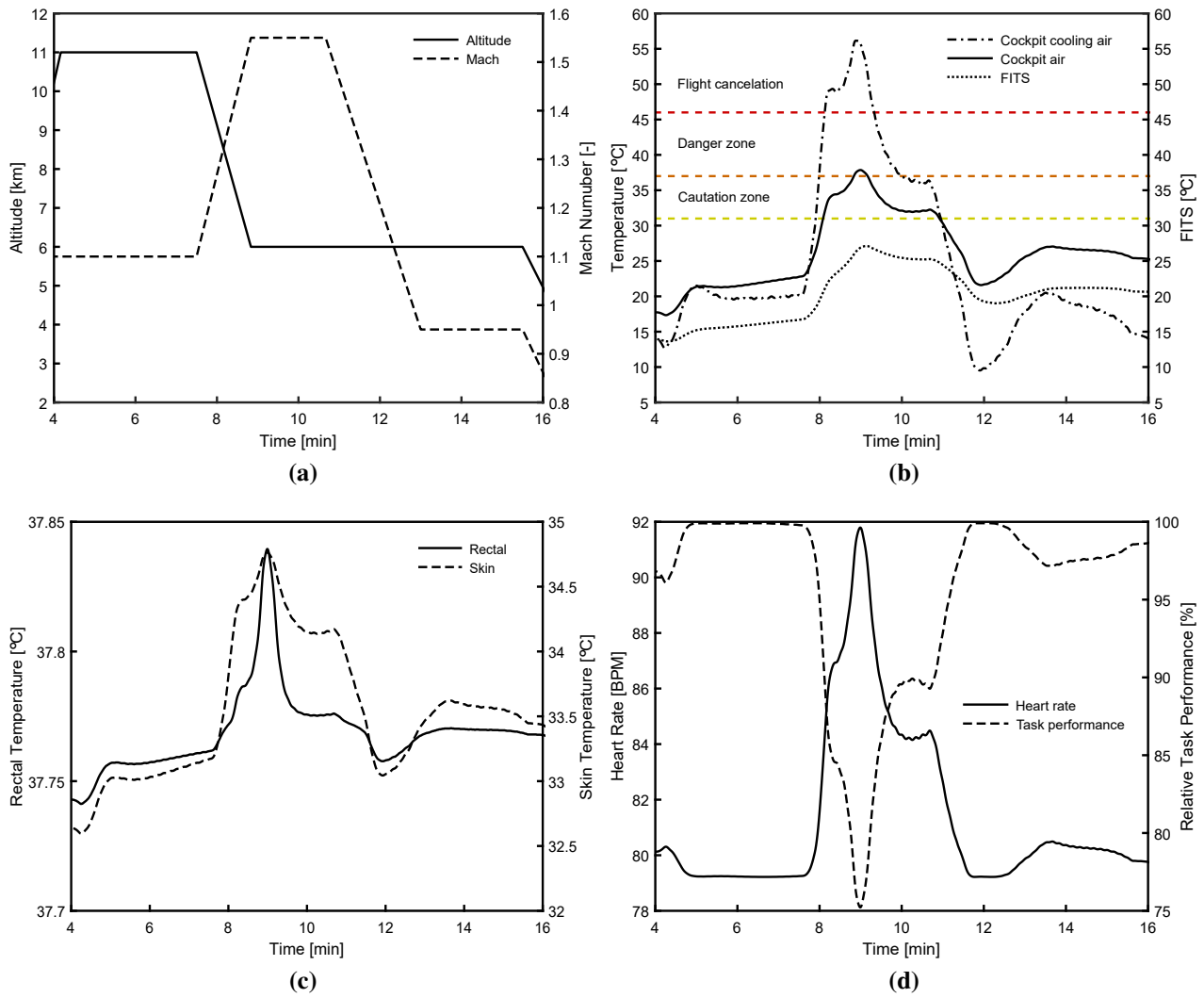
Fig. 4 : Transient simulation of cockpit air temperature and the impact on pilots physiological and psychological performance. **(a)**, generic flight with changing Mach number and altitude. **(b)**, impact of cooling and cockpit air temperature on FITS with Stribley [18] suggested FITS limits illustrating different flight risks which are not exceeded. **(c)**, predicted pilot skin temperature show larger changes compared to rectal temperature which maintains nearly constant. **(d)**, heard-rate and relative task performance behave contrary at increased cockpit temperatures.

heart rate (Fig.4d) respond with increased amplitudes when cockpit temperature is reaching its maximum. The skin temperature and heart rate show more distinct changes while rectal temperature only rises minimally. This result is expected since the skin has more direct contact with the cockpit air, while the stressed heart rate is a in vivo reaction attempting to remove heat from the body to maintain a constant core temperature that is close to rectal temperature [30]. Furthermore, mental performance drops with increased body heat load, and as a consequence so does the relative task performance of the pilot (Fig.4d).

The results also demonstrate that the modeling approach to connect smaller, one dimensional, independently running models via the FMI standard into a larger aircraft system simulator is very beneficial. On the one hand it provides a high compatibility of various simulation models and on the other hand a more heliocentric picture of the aircraft systems and their interactions. In addition, the FMI standard provides engineers

with the freedom to choose the optimal simulation tool for their particular problem without running into danger not being able to collaborate.

In summary, it can be said that the presented ASS seems to be functional for thermal comfort studies and shows reasonable results, yet refinements of the simulator and its sub-models continues and validation will follow.

5 Conclusion

Based on the presented results it can be concluded that the demonstrated aircraft system simulator has the potential to determinate various heat stress parameters supporting pilots in their flight preparation, increasing error awareness and thereby minimizing in-flight incidents. Moreover, it enables engineers to incorporate cockpit thermal comfort into the development of interfacing sub-systems in early design phases. Thereby design errors caused by possible sub-optimizations can be minimized.

6 Acknowledgements

7 Contact Author Email Address

Mail to: jorg.schminder@liu.se

Copyright Statement

References

[1] Standard. ASHRAE 55 - Thermal Environmental Conditions for Human Occupancy . Tech. rep., American Society of Heating, Refrigerating and Air Conditioning Engineers, Atlanta, US, 2017.

[2] Jessen C. *Temperature regulation in humans and other mammals*. Berlin : Springer, cop. 2001, 2001.

[3] Gaoua N. Cognitive function in hot environments: A question of methodology. *Scandinavian Journal of Medicine & Science in Sports*, vol. 20, no. Suppl 3, pp. 60 – 70, 2010.

[4] Nunneley S A, Stribley R F and Allan J R. Heat stress in front and rear cockpits of F-4 aircraft. *Aviation Space and Environmental Medicine*, vol. 52, no. 5, pp. 287–290, 1981.

[5] Reardon M, Fraser B and Omer J. Physiological Effects of Thermal Stress on Aviators Flying a UH-60 Helicopter Simulator. *Military Medicine*, vol. 163, no. 5, pp. 298–303, 1998.

[6] FMI development group. Functional Mock-up Interface for Model Exchange and Co-Simulation. Report 2.0, Modelica Association, 2014.

[7] Hällqvist R, Braun R and Krus P. Early Insights on FMI-based Co-Simulation of Aircraft Vehicle Systems. *Proceedings of 15:th Scandinavian International Conference on Fluid Power*, pp. 262–270. Linköping, 2017.

[8] Hällqvist R, Schminder J, Eek M, Braun R, Gårdhagen R and Krus P. A Novel FMI and TML-Based Desktop Simulator for Detailed Studies of Thermal Pilot Comfort. *31st Congress of the International Council of the Aeronautical Sciences*. Belo Horizonte, Brazil, 2018.

[9] Standard. ISO 2533:1975 - Standard Atmosphere. Tech. rep., International Organization for Standardization, Geneva, CH, 1975.

[10] Ananthasayanam M R and Narasimha R. A proposed International Tropical Reference Atmosphere up to 80 km. *Advances in Space Re-*

search, vol. 5, no. 7, pp. 145–154, 1985.

[11] Zuppardo J C. Graphical comparison of U.S. tandrd atmosphere and military standard climatic extremes. Tech. rep., Aeronautical Systems Center, 1993.

[12] Dymola Systems Engineering. https://www.3ds.com/products-services/catia/products/dymola/. Accessed: 2018-06-21.

[13] Fritzson P, Aronsson P, Lundvall H, Nyström K, Pop A, Saldamli L and Broman D. The Open-Modelica Modeling, Simulation, and Software Development Environment. *Simulation News Europe*, vol. 44, pp. 8–16, 2005.

[14] Shetty J, Lawson C and Shahneh A. Simulation for temperature control of a military aircraft cockpit to avoid pilot's thermal stress. *CEAS Aeronautical Journal*, vol. 6, no. 2, pp. 319–333, 2015.

[15] Jordan P and Schmitz G. A Modelica Library for Scalable Modelling of Aircraft Environmental Control Systems. *Proceedings of the 10th International Modelica Conference*. Lund, Sweden, 2014.

[16] Schminder J and Gårdhagen R. A generic simulation model for prediction of thermal conditions and human performance in cockpits. *Building and Environment*, vol. 143, pp. 120 – 129, 2018.

[17] Standard. ISO 7243:2017 - Ergonomics of the thermal environment - Assessment of heat stress using the WBGT (wet bulb globe temperature) index. Tech. rep., International Organization for Standardization, Geneva, CH, 2017.

[18] Stribley R F and Nunneley S A. Fighter Index of Thermal Stress: Development of Interim Guidance for Hot-Weather USAF Operation. Tech. rep., USAF School of Aerospace Medicine, Aerospace Medical Division, 1978.

[19] *ASHRAE Handbook Fundamentals*. 1st ed. American Society of Heating, Refrigerating, and Air-Conditioning Engineers, 1993.

[20] Standard. ISO 7730:2005 - Ergonomics of the thermal environment - Analytical determination and interpretation of thermal comfort using calculation of the PMV and PPD indices and local thermal comfort criteria. Tech. rep., International Organization for Standardization, Geneva, CH, 2005.

[21] Lind A R. A physiological criterion for setting thermal environmental limits for everyday work. *Journal of Applied Physiology (0021-8987)*, vol. 18, no. 1, p. 51, 1963.

[22] Song B, Cao X and Mitsui Y. A study of effect of Cockpit Heat Stress on Pilot Thermal Strain. *Japan Society for Aeronautical and Space Sciences*, vol. 38, no. 119, pp. 57–65, 1995.

[23] Luo M, Zhou X, Zhu Y and Sundell J. Revisiting an overlooked parameter in thermal comfort studies, the metabolic rate. *Energy and Buildings*, vol. 118, pp. 152 – 159, 2016.

[24] Seppänen O, Fisk W J and Lei Q. Effect of temperature on task performance in office environment. Tech. rep., Helsinki University of Technology, Laboratory for Heating Ventilating and Air-conditioning, 2006.

[25] Ramsey J, Burford C, Beshir M and Jensen R. Effects of Workplace Thermal Conditions on Safe Work Behavior. *Safety Research*, vol. 14, pp. 105 – 114, 1983.

[26] FMI tools for Simulink - FMI Kit. https://www.3ds.com/products-services/catia/products/dymola/fmi/. Accessed: 2018-06-28.

[27] Open Cyber-Physical System Model-Driven Certified Development (OpenCPS). https://opencps.eu/. Accessed: 2018-06-28.

[28] Kuhta S F, Clark J W, Gillies W J, Climpson C R, Dandridge L A and Slodkowski L I. F/A-18E/F will Provide Marginal Operational Improvement at High Cost . Tech. rep., United States General Accounting Office, Washington D.C., US, 1996.

[29] SAAB-Scania. Fpl AJ 37 Speciell Förarinstruktion (SFI) Komplement Del 3 (M7780-400173). Tech. rep., Försvarets Materielverk, Stockholm, Sweden, 1979.

[30] Wyss C, Brengelmann G, Johnson J, Rowell L and Niederberger M. Control of skin blood flow, sweating, and heart rate: role of skin vs. core temperature. *Applied Physiology*, vol. 36, no. 6, pp. 726–733, 1974.